Global Biogeochemical Cycles®

RESEARCH ARTICLE
10.1029/2026GB009114

Revisiting the Ocean's Metabolic Balance: Correcting Biases in Bottle Incubations Reveals a More Autotrophic and Dynamic Ocean

Yao Liu[1,2], Yibin Huang[1,3], Mingwang Xiang[1,2,4], Junjie Zhou[1,2], Bingzhang Chen[5], Nicolas Cassar[6], Weilei Wang[1,3], and Bangqin Huang[1,2]

[1]State Key Laboratory of Marine Environmental Science, Xiamen University, Xiamen, China, [2]National Observation and Research Station for the Taiwan Strait Marine Ecosystem, College of the Environment and Ecology, Xiamen University, Xiamen, China, [3]College of Ocean and Earth Sciences, Xiamen University, Xiamen, China, [4]Guangxi Key Laboratory of Beibu Gulf Marine Resources, Environment and Sustainable Development, Fourth Institute of Oceanography, Ministry of Natural Resources, Beihai, China, [5]Department of Mathematics and Statistics, University of Strathclyde, Glasgow, UK, [6]Division of Earth and Ocean Sciences, Nicholas School of the Environment, Duke University, Durham, NC, USA

Abstract The ocean's metabolic state—reflecting the balance between organic carbon production and consumption—is fundamental to understanding carbon sequestration potential. Yet, whether the ocean is net autotrophic or heterotrophic remains actively debated. Classic light-dark bottle incubations often suggest net heterotrophy, whereas geochemical tracer-based assessments indicate widespread autotrophy. Here, we show that bottle incubations systematically overestimate heterotrophy by artificially exacerbating bacterial activity, especially in oligotrophic waters. Applying a correction to global incubation data reduces the fraction of areas exhibiting net heterotrophy from 66% to 12% and shifts the euphotic zone carbon budget from a deficit of -9 ± 2.4 Pg C yr^{-1} to a surplus of $+12 \pm 3.5$ Pg C yr^{-1}. Moreover, our revisited estimate reveals that oligotrophic gyres are seasonally dynamic, oscillating between net autotrophy and heterotrophy, yet remain net autotrophic on an annual scale. These results help partly reconcile the long-standing methodological discrepancy in ocean metabolic balance and highlight the need to reassess biologically mediated carbon flux estimates in other aquatic systems broadly reliant on incubation-based measurements.

Plain Language Summary For decades, the ocean's metabolic balance has been obscured by conflicting methodological approaches, fueling debate over whether the global ocean is a net biogenic carbon source or sink. By identifying and correcting systematic biases in classic incubation-based measurements, our study reconciles this long-standing discrepancy and reveals that oligotrophic oceans, while seasonally dynamic, are net autotrophic on an annual scale—aligning with nonincubation-based assessments. These findings provide new insights into a central controversy in ocean biogeochemistry and call for a broad reassessment of incubation-based respiration estimates across aquatic ecosystems.

Key Points:

- Bottle incubations overestimate heterotrophy by stimulating bacterial respiration, especially in oligotrophic waters
- Correcting this bias shifts global ocean net community production from −9 to +12 Pg C yr^{-1} and reduces heterotrophic area from 66% to 12%
- Oligotrophic gyres are seasonally variable but annually net autotrophic, reconciling incubation and tracer-based estimates

Supporting Information:

Supporting Information may be found in the online version of this article.

Correspondence to:

Y. Huang and B. Huang,
yibin.huang@xmu.edu.cn;
bqhuang@xmu.edu.cn

Citation:

Liu, Y., Huang, Y., Xiang, M., Zhou, J., Chen, B., Cassar, N., et al. (2026). Revisiting the ocean's metabolic balance: Correcting biases in bottle incubations reveals a more autotrophic and dynamic ocean. *Global Biogeochemical Cycles*, *40*, e2026GB009114. https://doi.org/10.1029/2026GB009114

Received 29 JAN 2026
Accepted 27 MAY 2026

Author Contributions:

Conceptualization: Yibin Huang, Bangqin Huang
Investigation: Yao Liu, Mingwang Xiang, Junjie Zhou
Methodology: Yibin Huang, Bingzhang Chen
Supervision: Yibin Huang, Bangqin Huang
Visualization: Yao Liu
Writing – original draft: Yao Liu, Yibin Huang
Writing – review & editing: Yibin Huang, Bingzhang Chen, Nicolas Cassar, Weilei Wang, Bangqin Huang

1. Introduction

The ocean is the Earth's largest active carbon reservoir, holding over 50 times the amount of carbon in the atmosphere, and plays a pivotal role in regulating the global carbon cycle and climate (DeVries, 2022; Falkowski et al., 2000). The ocean metabolic state, defined as the balance between organic matter production and respiration consumption, is a key metric for evaluating the upper-ocean carbon budget and ecosystem health (Ducklow & Doney, 2013). In net autotrophic systems, the organic matter produced in excess of consumption is available for export to the deep ocean for long-term biogenic carbon sequestration. Conversely, ecosystems can be temporarily net heterotrophic, or rely on external organic matter inputs to meet metabolic demands, rendering them more susceptible to external forcing such as organic matter transport pathways.

Despite its fundamental importance, the global ocean's metabolic balance, especially in oligotrophic regions, remains actively debated (Duarte et al., 2013; Ducklow & Doney, 2013; Williams et al., 2013). This controversy largely arises from methodological discrepancies in measuring euphotic-zone integrated net community production (NCP), a key metric for quantifying marine ecosystems' metabolic balance and, when integrated over sufficiently long timescales and assuming near steady state, also serves as a proxy for organic carbon export. NCP estimates derived from budgeting of in situ biogeochemical tracers such as oxygen, nitrate, or dissolved inorganic

carbon, or from numerical or empirical satellite models, typically suggest a net autotrophic state on an annual scale (Huang et al., 2022a, 2023; Siegel et al., 2023; Wang et al., 2023). In contrast, NCP estimates derived from the classic light-dark bottle incubation method often indicate widespread net heterotrophy in the oligotrophic oceans (Duarte & Agustí, 1998; Duarte et al., 2013; Westberry et al., 2012). For instance, a year-long measurement from bottle incubations at station ALOHA in the North Pacific Subtropical Gyre reported a net heterotrophic state with a net carbon deficit of −9 mol O_2 m^{-2} yr^{-1} (Williams et al., 2004). Similarly, bottle-based measurements during the Atlantic Meridional Transect cruises found net heterotrophy in both northern and southern subtropical gyres, with deficits of −32.3 and −38.9 mol O_2 m^{-2} yr^{-1}, respectively (Serret et al., 2002). Extrapolated globally, bottle incubation results imply that more than half of the ocean is net heterotrophic (Duarte & Agustí, 1998; Duarte et al., 2013). It is particularly difficult to reconcile with observations of net organic carbon export to the ocean interior and mesopelagic carbon demand (Burd et al., 2010)—unless compensated by an advective supply of organic carbon. This discrepancy highlights the urgent need for methodological reconciliation.

Light-dark bottle incubations measure NCP by tracking changes in dissolved oxygen (DO) over 24 hr, calculating gross primary production (GPP), community respiration (CR), and their difference as NCP (Ducklow & Doney, 2013). However, growing evidence suggests that the net heterotrophic signals often reported in bottle-based studies may result from an overestimation of CR. For instance, bottle-derived CR in the North Atlantic Subtropical Gyre exceeded theoretical estimates based on plankton biomass and growth efficiency by up to 48% (Morán et al., 2007). Similarly, observations from the Northwest Pacific indicate that light bottle-derived GPP closely matched biogeochemical model predictions, whereas CR significantly exceeded empirical respiration estimates of major planktonic groups by about 30% (Huang et al., 2019). More recently, work demonstrated that bacterial activity increased significantly after 24-hr bottle confinement (Guo et al., 2022). Since bacteria are major contributors to ocean respiration (Azam, 1998; García-Martín et al., 2017; Heneghan et al., 2024), this artificial boost in bacterial activity could explain the overestimation of CR and, consequently, the underestimation of NCP in light-dark bottle measurements. However, the quantitative impact of enhanced bacterial activity during incubation on CR and the resulting metabolic balance assessments remains poorly understood. Here, we comprehensively assess bottle effects on bacterial activity and metabolic balance across coastal-to-oligotrophic gradients through five field expeditions. We further introduce a conceptual framework to quantify incubation-driven bacterial activity changes and their impact on respiration and NCP estimates. By integrating this correction into a global bottle incubation data set, we revisit NCP estimates, helping reconcile long-standing methodological inconsistencies between bottle-based and non-bottle-based approaches and advancing our understanding of the ocean's metabolic state (Figure 1).

2. Materials and Methods

2.1. Metabolic State Derived From the Light-Dark Bottle Incubations

Field measurements were conducted in the marginal seas of the Northwest Pacific, covering a broad environmental gradient from coastal to oligotrophic regimes. Sampling took place during five cruises between 2018 and 2023, spanning 66 stations (Figure 1a and Figure S1 in Supporting Information S1). Surface seawater samples (3–5 m depth) were collected using Niskin bottles, and metabolic state assessments followed the classic light-dark bottle method described in previous studies (Serret et al., 2001; Williams et al., 2004). Our primary goal was to incorporate bacterial respiration (BR) bias corrections into previous global bottle-based metabolic balance estimates to determine whether this correction helps narrow the methodological discrepancies in metabolic state measurements between bottle-based and non-bottle-based approaches, rather than focusing on the exact mechanisms causing the bottle effect (e.g., the effect of different bottle sizes). To ensure comparability with existing global bottle incubation data sets and facilitate global corrections, we intentionally selected 100-mL biochemical oxygen demand (BOD) bottles, as they represent the most commonly used standard volume range (75–120 mL) in previous studies (Robinson & Williams, 2005). At each station, surface seawater was gently siphoned into BOD bottles. Four bottles were immediately fixed with Winkler reagents. Four light bottles were exposed to natural irradiance, whereas four dark bottles were wrapped with opaque material to exclude light and incubated alongside light bottles in a temperature-controlled seawater tank. Continuous seawater circulation using surface seawater pumped directly from the sampling site maintained all bottles at near in situ temperature, minimizing potential thermal differences between treatments. Therefore, any temperature-related artifacts associated with light and dark shielding are considered negligible. All incubations were conducted over a 24-hr period, representing the

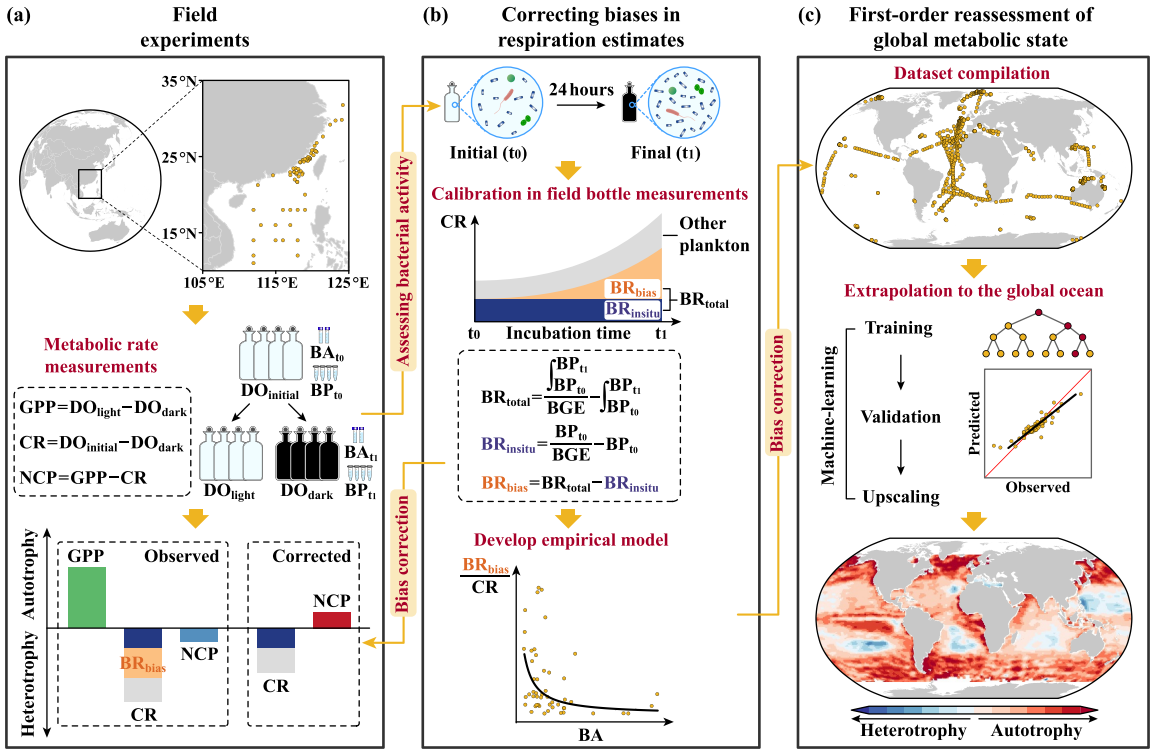

Figure 1. Conceptual framework of the study. (a) Field experiments to measure the metabolic balance using the classic light-dark bottle incubation in the Northwest Pacific marginal seas, with simultaneous collection of bacterial metabolic parameters before and after incubation to track dynamic changes in bacterial activity. Net community production (NCP) is calculated as the difference between gross primary production (GPP, calculated as the dissolved oxygen (DO) in light bottles minus DO in dark bottles after 24 hr of incubation) and community respiration (CR, calculated as the difference between initial DO and DO in dark bottles after incubation). (b) A new framework that integrates relative changes in bacterial production (BP, measured by ^{3}H-leucine incorporation rate) with bacterial growth efficiency to quantitatively assess the additional respiration induced by bottle confinement and its impact on CR estimates. (c) First-order reassessment of global metabolic balance from our compilation of the light-dark bottle data set. Using empirical relationships between respiration biases and environmental factors derived from our field experiments, we calculated overestimations in respiration due to bacterial activity changes in each sample of the data set. We then corrected the original NCP estimates by subtracting these bacterial-induced respiration biases to generate a first-order correction of NCP from bottle incubations. A machine-learning model is applied to extrapolate the corrected NCP globally. See Methods for details. BA: bacterial abundance; t_0: initial time (0-hr); t_1: time at the end of incubation (24-hr); BR_{insitu}: actual in situ bacterial respiration (BR); BR_{bias}: overestimated respiration caused by artificially enhanced bacterial activity during bottle incubation; BR_{total}: total BR observed in bottle-based measurements, equal to the sum of BR_{insitu} and BR_{bias}.

standard duration used in light-dark bottle experiments to resolve diel metabolic balance and capture both production and respiration processes (Huang et al., 2021; Westberry et al., 2012). After 24 hr, DO concentrations were measured in four bottles from each group. GPP, CR, and NCP were calculated using the following equations (Equations 1–3):

$$GPP = DO_{light} - DO_{dark} \quad (1)$$

$$CR = DO_{initial} - DO_{dark} \quad (2)$$

$$NCP = GPP - CR = DO_{light} - DO_{initial} \quad (3)$$

Here, $DO_{initial}$, DO_{dark}, and DO_{light} represent the mean DO concentrations in the BOD bottles at the initial time, and in the dark and light bottles after 24 hr of incubation, respectively.

2.2. Assessing Bacterial Activity During the Incubation

To evaluate changes in bacterial activity during bottle incubation, bacterial abundance (BA) and bacterial production (BP) were measured from the initial bottle (representing in situ conditions) and dark bottle after 24-hr incubation (Figure 1a). BA was quantified using an Accuri C6 flow cytometer (Becton Dickinson, USA) (Marie et al., 2005). BP was quantified using the ^{3}H-leucine incorporation method (Kirchman, 2001). Leucine

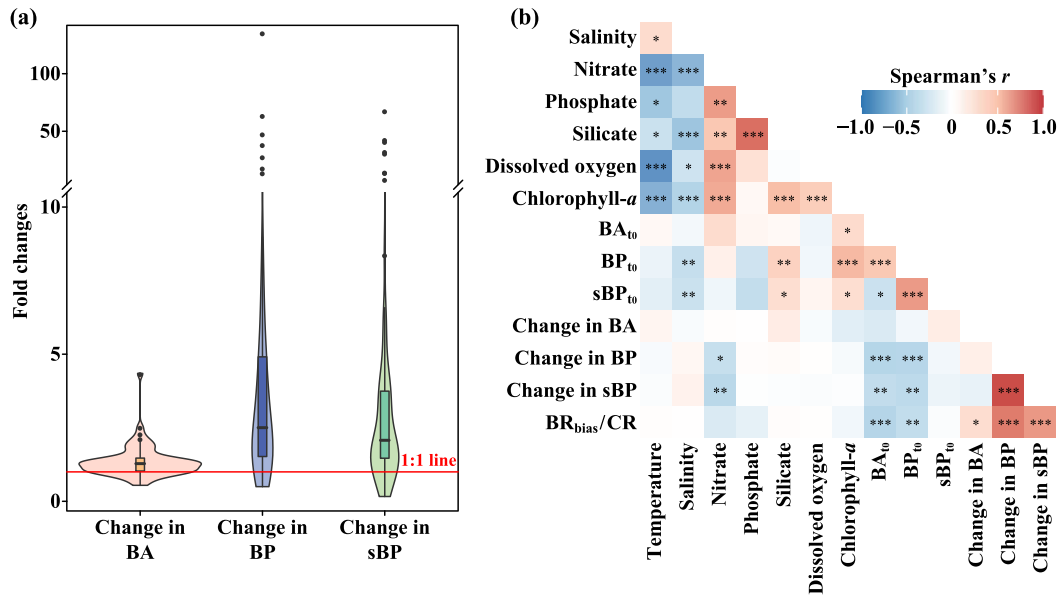

Figure 2. Changes in bacterial activity before and after incubation and their relationships with environmental factors. (a) Growth multiples of bacterial abundance (BA), bacterial production (BP), and cell-specific BP (specific bacterial production) before and after incubation based on 66 incubation experiments conducted along a coastal-to-oligotrophic gradient. Presented as violin plots showing the distribution of multiples, and the red horizontal line represents the 1:1 line (no change in bacterial activity over the incubation period). (b) Correlations between bacterial activity changes and environmental factors. Significant levels: $*p < 0.05$, $**p < 0.01$, and $***p < 0.001$. BA_{t0}, BP_{t0}, and sBP_{t0} denote initial BA, BP, and cell-specific BP at the start of incubation, respectively; CR: community respiration; BR_{bias}: overestimated respiration caused by artificially enhanced bacterial activity during bottle incubation.

incorporation rates were converted to carbon units using a conversion factor of 0.37 kg C mol leucine^{-1}, derived from prior studies in our study region (Huang et al., 2019; Wang et al., 2014). As a complementary approach to examine the time-dependent growth dynamics of bacterial activity under incubation conditions, BA and BP were monitored in parallel every 4 hr over a 24-hr incubation period at three additional stations (Figure S2 in Supporting Information S1).

2.3. A Conceptual Framework to Quantify Bias in Respiration Estimates

We observed a clear and significant increase in bacterial activity, as indicated by both BA and BP within the bottle incubation system (Figure 2a and Figure S3 in Supporting Information S1; see Results and Discussion section). Assuming that BR scales with bacterial activity, this enhancement is expected to lead to an overestimation of CR in bottle-based measurements. To address this bias, we developed a model that integrates changes in BP, combined with bacterial growth efficiency (BGE), to quantify the additional BR caused by enhanced bacterial activity during incubation. The framework and specific calculations are described below (Figure 1b).

The total CR observed in dark bottles over 24 hr reflects contributions from phytoplankton, zooplankton, and bacteria. When bacterial activity is artificially enhanced during the incubation, total BR (BR_{total}) can be partitioned into two components (Equation 4):

$$BR_{total} = BR_{insitu} + BR_{bias} \quad (4)$$

where BR_{insitu} is the actual in situ BR, and BR_{bias} represents the overestimated respiration due to confinement-induced bacterial activity. The magnitude of BR can theoretically be inferred from BP and BGE (Equation 5) (Robinson & Williams, 2005):

$$BR = \frac{BP}{BGE} - BP \quad (5)$$

Substituting this expression in Equation 4 gives:

$$BR_{bias} = \underbrace{\left(\frac{BP_{total}}{BGE} - BP_{total}\right)}_{BR_{total}} - \underbrace{\left(\frac{BP_{insitu}}{BGE} - BP_{insitu}\right)}_{BR_{insitu}} \quad (6)$$

where BP_{insitu} corresponds to the actual in situ BP at the start of the incubation (BP_{t0}), while BP_{total} represents the time-integrated BP over 24 hr, including both the initial production and the increase caused by confinement effects. In closed systems, bacterial biomass and metabolic rates often exhibit exponential growth over time (Guo et al., 2022; Pomeroy et al., 1994), a pattern further confirmed by the high-frequency time-series observations in our study (Figure S2 in Supporting Information S1). Thus, BP_{total} can be expressed as an exponential integral (Equation 7):

$$BP_{total} = \int_{t0}^{t1} BP_{t0} e^{rt} dt = \frac{BP_{t0}(e^{rt} - 1)}{r} \quad (7)$$

where e represents the base of the natural logarithm, r is the exponential growth rate of bacterial activity, derived from the initial (BP_{t0}) and final (BP_{t1}) BP values measured over the incubation period (t) (Equation 8):

$$r = \frac{\ln \frac{BP_{t1}}{BP_{t0}}}{t} \quad (8)$$

To improve calculation accuracy, BGE was experimentally determined for each station (Text S1 and Figure S4 in Supporting Information S1). The assumption of relatively constant BGE during incubation were verified by additional experiments at some specific stations combined with theoretical derivation (Text S2 in Supporting Information S1), ensuring a robust linkage between changes in bacterial activity and BR. Furthermore, although BP estimates depend on the choice of leucine-to-carbon conversion factors, this dependency does not propagate into the quantification of BR_{bias} (see Text S3 in Supporting Information S1). Together, robust estimates of BGE and BP enable reliable quantification of BR_{bias}. Finally, BR_{bias} was applied to correct the NCP values, yielding a more accurate estimate of the metabolic state (Equation 9):

$$NCP_{corr} = NCP + BR_{bias} \quad (9)$$

2.4. First-Order Correction of NCP for Global Light-Dark Bottle Data set

To evaluate the global impact of overestimated BR on previous bottle-based metabolic balance estimates, we compiled a global light-dark bottle incubation data set (Figure 1c). This data set extends the compilation by Huang et al. (2021) by incorporating more observations. All measurements in this data set were conducted using 24-hr incubations and bottle volumes within the standard range (75–120 mL). This methodological consistency ensures compatibility with our incubation experiments, allowing the empirical relationships derived in this study to be applied to the global data set in a first-order sense. Observations missing critical metadata (e.g., location, time, GPP, CR, or NCP values) or unsuitable for euphotic depth integration were excluded. The data set comprised 3,188 observations from 749 stations, spanning a wide range of ecological conditions across the global ocean. Field observations showed that the ratio of overestimated BR to the measured CR (BR_{bias}/CR) was significantly and negatively correlated with in situ BA (Figure 2b; see Results and Discussion section). Building on this relationship, we sought to develop an empirical model to quantify the effect of bottle-confinement-enhanced bacterial activity on CR, enabling its application to larger oceanic areas for NCP adjustments (Equation 10; Figure S5 in Supporting Information S1):

$$\frac{BR_{bias}}{CR} = \frac{1}{1 + 10^{1.083(\pm 0.311)\log_{10}BA - 5.554(\pm 1.818)}} \quad (10)$$

The empirical model developed above (Equation 10) was then applied to the global light-dark bottle data set. For each sampling depth at each station, we obtained the BA by matching it with the global gridded BA product (Buitenhuis et al., 2012) based on sampling locations and depths. Then BR_{bias} was calculated for each water layer, and the corrected NCP value was computed by adding the estimated respiration bias to the originally reported NCP value (Equation 11):

$$NCP_{corr} = NCP + \underbrace{\frac{BR_{bias}}{CR} \cdot CR}_{BR_{bias}} \tag{11}$$

Finally, volumetric NCP values (both corrected and uncorrected) were integrated above the euphotic zone at each station using the trapezoidal integration method to obtain depth-integrated values.

2.5. Extrapolation the Revised NCP to the Global Ocean

A machine-learning approach was applied to extrapolate corrected and uncorrected NCP values to the global ocean. To reduce the impact of spatial autocorrelation during algorithm training, the global euphotic zone-integrated NCP data were first aggregated into 1° × 1° monthly climatological grids, resulting in 292 grid points. Each grid point was then matched with a suite of environmental predictors. We initially included a broad suite of environmental predictors that directly and indirectly affect NCP dynamics—and then assessed multicollinearity using the variance inflation factor (VIF). Predictors with VIF > 5 were removed to avoid redundancy. The final set of variables retained for model training included temperature, salinity, DO, and nutrient concentrations (e.g., silicate, nitrate) from the World Ocean Atlas 2023; mixed-layer depth from HYCOM; and sea-surface chlorophyll and primary production derived from satellite observations (Table S1 in Supporting Information S1). To ensure numerical continuity in both spatial and temporal dimensions, latitudes, longitudes, and months were converted into periodic functions (Yu et al., 2024). We constructed separate machine-learning models for corrected and uncorrected NCP data sets using the Random Forest algorithm, implemented via the "randomForest" *R* package. The 292 grid points were divided into 70% training data and 30% validation data. Default parameters, including 500 decision trees and a minimum leaf size of 3, were used for model construction. Model performance was evaluated by comparing observed and predicted values in the validation data set using the coefficient of determination (R^2) and root mean square error metrics (Figure S6 in Supporting Information S1). The established machine-learning models were applied to global gridded (1° × 1°) environmental data sets to produce monthly climatological NCP maps. The final NCP climatology spans 65°S–65°N, with high-latitude sea-ice regions and grids with extensive data gaps excluded from the analysis.

2.6. Uncertainty Estimation

We quantified uncertainty in our global NCP predictions by propagating three primary error sources: (a) measurement error in NCP (standard errors reported in the compiled data set), (b) fitting error in the empirical respiration-bias correction (Equation 10; Figure S5 in Supporting Information S1), and (c) machine-learning algorithm (training data set composition and hyperparameter choice). Using a Monte Carlo framework with 1,000 iterations, we first perturbed each original NCP value by adding a random draw from a normal distribution whose standard deviation equaled its measurement error. We then perturbed the respiration-bias correction by sampling deviations for each regression coefficient from normal distributions defined by their fitting uncertainties and applied the updated correction to NCP. Next, we resampled the training data (with the perturbed NCP values) and randomly sampled the Random Forest hyperparameters—ntree from 100 to 1,000 and mtry from the integer range $(\sqrt{p} - 2)$ to $(\sqrt{p} + 2)$, where p is the number of predictors. At each iteration, we generated a global NCP prediction; the mean of the 1,000 simulations was taken as the final estimate, and the standard deviation across iterations was reported as the propagated uncertainty.

2.7. Comparison With Independent Estimates of NCP and Carbon Export

Our revised global NCP was compared with O_2/Ar-derived NCP (Li & Cassar, 2016) and three independent carbon export estimates: hydrographic inverse model (Wang et al., 2023), food-web model (Siegel et al., 2014), and satellite-derived net primary production scaled by empirical ^{234}Th-based carbon export ratios (*f*-ratio) (Henson et al., 2011). We also included NCP estimates from Biogeochemical-Argo observations across major

open-ocean regions (Izett et al., 2024). To ensure comparability across methods, all C:O ratios were converted using a factor of 1:1.4 (Laws, 1991).

3. Results and Discussion

3.1. Stimulatory Effects of Bottle Incubations on Bacterial Activity

We assessed bacterial activity changes during bottle incubations by comparing BA and BP before (0-hr) and after (24-hr) incubation across 66 experiments spanning diverse environmental gradients (Figure 1a and Figure S1 in Supporting Information S1). After 24 hr, BA across all stations increased by a median of 1.3-fold relative to initial values, while BP showed a substantially greater increase, with a median of 2.5-fold (Figure 2a and Figure S3 in Supporting Information S1). High-frequency sampling (every 4 hr) at selected stations revealed that the increase in BA and BP in the bottle generally followed an exponential trend (Figure S2 in Supporting Information S1), consistent with previous studies (Guo et al., 2022; Pomeroy et al., 1994). The disproportionate rise in BP relative to BA indicates that enhanced bacterial activity is driven not only by higher cell numbers but also by elevated metabolic potential, as further supported by a 2.1-fold median increase in cell-specific BP (specific bacterial production (sBP)) (Figure 2a and Figure S3 in Supporting Information S1).

These stimulatory effects likely result from resource redistribution, trophic cascades, and shifts in bacterial community structure. For example, mortality of plankton or viral lysis may release dissolved organic carbon (DOC) and nutrients (Calvo-Diaz et al., 2011; Moran et al., 2022), fueling bacterial growth during incubation. The enclosed environment may accelerate DOC diffusion and recycling, favoring "opportunistic copiotrophs" that rapidly exploit organic matter (Baltar et al., 2012; Massana et al., 2001). Additionally, bottle walls provide favorable surfaces for the growth of attached bacteria (Alotaibi, 2021; Qian et al., 2022), which typically exhibit higher metabolic activity and faster growth rates, further contributing to the observed increase in bacterial activity (Baumas et al., 2021). Unintentional introduction of external DOC during experimental setup may also drive bacterial activity above natural in situ levels.

Our study region, spanning nutrient-rich coastal waters to oligotrophic basins, allows us to assess environmental influences on these effects. We found that changes in BP and sBP are negatively correlated with in situ nitrate concentrations (BP: $r = -0.34$, $p < 0.05$; sBP: $r = -0.42$, $p < 0.01$), BA (BP: $r = -0.44$, $p < 0.001$; sBP: $r = -0.37$, $p < 0.01$), and BP levels (BP: $r = -0.43$, $p < 0.001$; sBP: $r = -0.39$, $p < 0.01$) (Figure 2b), indicating that bacterial activity is more strongly stimulated in low-productivity systems such as oligotrophic gyres. In the oligotrophic ocean, limited organic substrates and microbial loop activity make bacterial communities more sensitive to resource shifts (Duan et al., 2021) and thus more susceptible to the effects induced by bottle incubation. The dominant picophytoplankton populations in these regions, such as *Prochlorococcus* and *Synechococcus*, exhibit high turnover and morality rates (Mojica et al., 2016; Pierella Karlusich et al., 2020), which may lead to a more rapid cycling of organic substrates during the incubation period relative to regions dominated by the classical grazing food web, where primary production more often passes to herbivorous zooplankton. Additionally, bacteria in oligotrophic environments often rely on proteorhodopsin-based phototrophy to mitigate carbon limitation (Gómez-Consarnau et al., 2019; Munson-McGee et al., 2022). Dark bottle incubations inhibit proteorhodopsin activity, forcing bacteria to rely on increased heterotrophic respiration to meet energy demands.

3.2. Quantitative Impact on Bacterial Respiration Biases

Our field observations reveal a significant enhancement of bacterial activity during bottle incubation, particularly in oligotrophic regions. As bacteria are major contributors to marine respiration (Azam, 1998; García-Martín et al., 2017; Heneghan et al., 2024), the observed increase in bacterial metabolic activity inevitably leads to elevated bacterial respiration (BR), which, in turn, results in an overestimation of CR in bottle-based measurements. To address this issue, we propose a conceptual framework that converts the 24-hr time-integrated increase in BP observed in bottles into confinement-induced excess BR using site-specific bacterial growth efficiency (BGE—the fraction of assimilated organic carbon partitioned to biomass rather than respired) (Figure 1b, see Methods section). We treat this excess as a systematic inflation of CR and correct the bottle-derived rates by subtracting it from CR (equivalently adding it to NCP), yielding estimates that better reflect in situ metabolic balance.

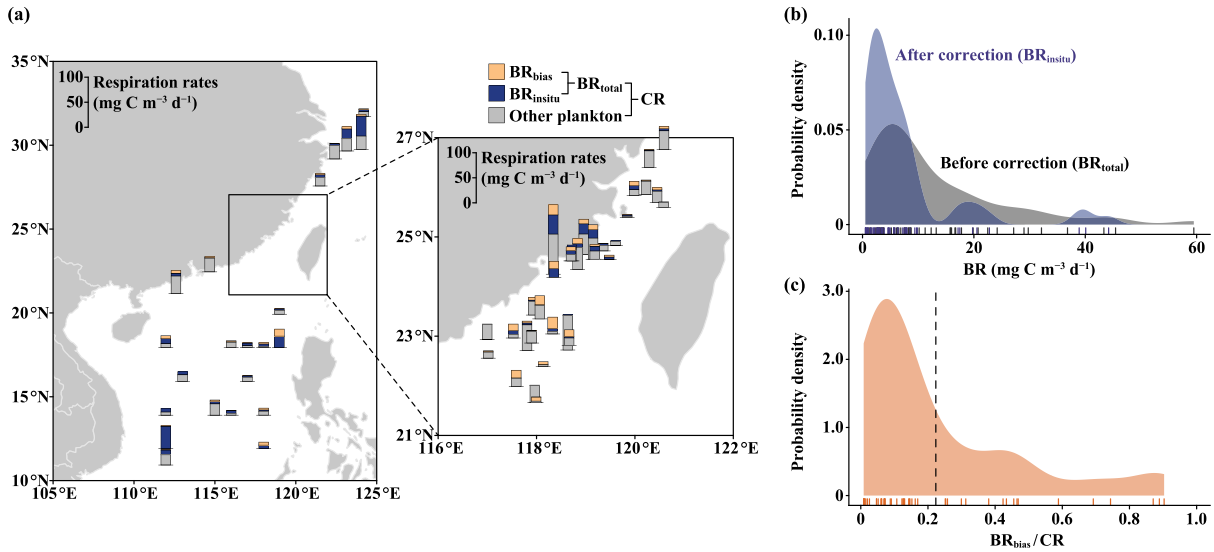

Figure 3. Quantification of bacterial respiration (BR) biases and their impacts on community respiration (CR) measurements. (a) Composition of CR measured in field studies. (b) Probability density distribution of BR before and after correction in bottle-based measurements. (c) Probability density distribution of the ratio of artificially enhanced BR to CR (BR_{bias}/CR). The rug plot displays each sample ($N = 66$), with the dashed line representing the mean of the distribution. BR_{insitu}: actual in situ BR; BR_{bias}: overestimated respiration caused by artificially enhanced bacterial activity during bottle incubation; BR_{total}: total BR observed in bottle-based measurements, equal to the sum of BR_{insitu} and BR_{bias}.

After correcting for confinement-induced stimulation, BR declined from 0.9 to 59.3 to 0.5–44.0 mg C m^{-3} d^{-1}—an average ~2-fold reduction (Figures 3a and 3b). The resulting bias, expressed as BR_{bias}/CR, averaged 22% across stations and exceeded 50% at some sites (Figure 3c). These findings align with previous results from Huang et al. (2019), which indicated that about 30% of the respiration measured by bottle incubations could not be accounted for by estimates based on regional plankton biomass and empirical growth efficiency in adjacent regions of the Northwest Pacific. This suggests that BR overestimation is a major contributor to unexplained respiration observed in bottle-based measurements. Correlation analyses further revealed significant negative relationships between BR_{bias}/CR and initial BA ($r = -0.44$, $p < 0.001$) and BP ($r = -0.36$, $p < 0.01$) (Figure 2b). Notably, correcting for the overestimation of BR results in previously negative NCP values shifting to positive at four stations (Figure S7 in Supporting Information S1). These results underscore the substantial impact of confinement-induced bacterial activity on metabolic balance assessments derived from light-dark bottle methods.

3.3. First-Order Correction of Global Metabolic State

Our field experiments show that bacterial activity enhancement during bottle incubation significantly biases respiration estimates, altering metabolic balance assessments derived from light-dark bottle measurements. To assess the global implications of this bias, we apply our empirically derived BR correction—based on observed relationships between respiration bias and environmental factors from our field experiments (modeled as a function of in situ BA; Equation 10)—to a global light-dark bottle data set (Figure 1c). The corrected NCP values are computed by adding the estimated respiration bias to the originally reported values, and then extrapolate globally using Random Forest machine-learning algorithms. It is important to note that this correction specifically addresses biases arising from bottle-induced bacterial activity changes. While other factors, such as phytoplankton and zooplankton responses, may also influence NCP estimates, direct measurement of their heterotrophic metabolism remains challenging and is not included in our analysis. Given that bacteria are the primary contributors to CR, and that the overestimation of BR aligns with unaccounted respiration from independent biomass-based approaches in the same region (Huang et al., 2019), we consider BR overestimation the dominant source of bias. Thus, our correction serves as a first-order adjustment.

Before correction, incubation-based estimates of global metabolic state upscaling using the Random Forest machine-learning approach suggest that approximately 66% of the global ocean is net heterotrophic, with the five subtropical gyres exhibiting persistent net heterotrophy year-round (Figures 4 and 5). After applying the first-order correction, the global proportion of net heterotrophic regions dropped dramatically to 12%, with most

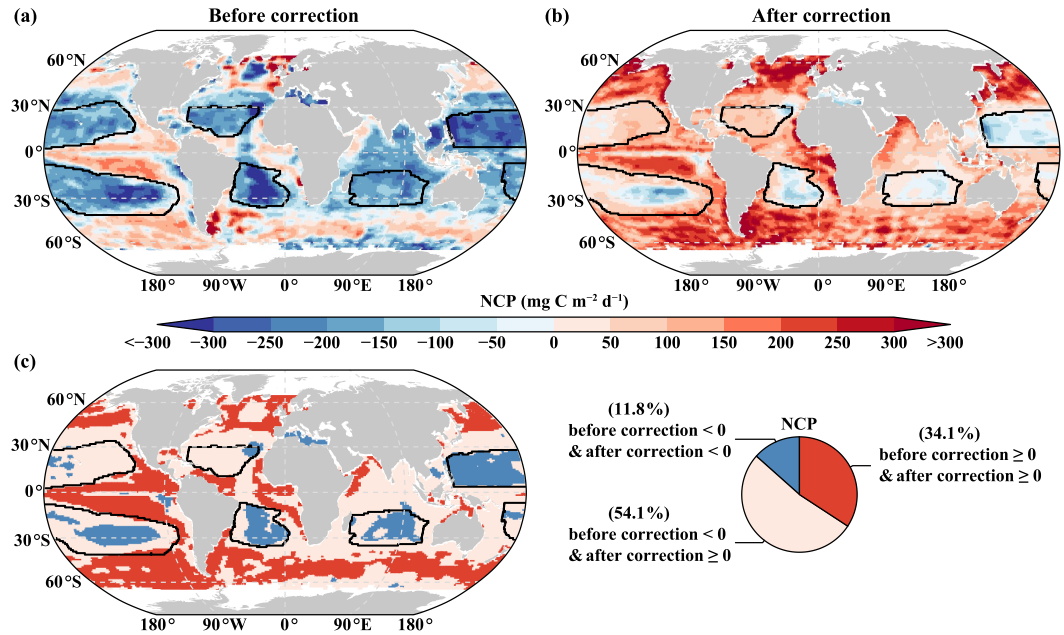

Figure 4. First-order reassessment of the global ocean's metabolic balance in the euphotic zone by correcting bacterial respiration (BR) biases. (a) Annual mean net community production (NCP) derived from uncorrected light-dark bottle measurements. (b) Annual mean NCP after correcting for BR overestimation caused by bottle confinement. (c) Changes in net autotrophic and heterotrophic regions before and after correction. Latitude range: 65°S–65°N. Subtropical oligotrophic gyres are defined by climatological chlorophyll-*a* concentrations <0.1 mg m^{-3} (Dai et al., 2023) and are indicated by black circles on the map.

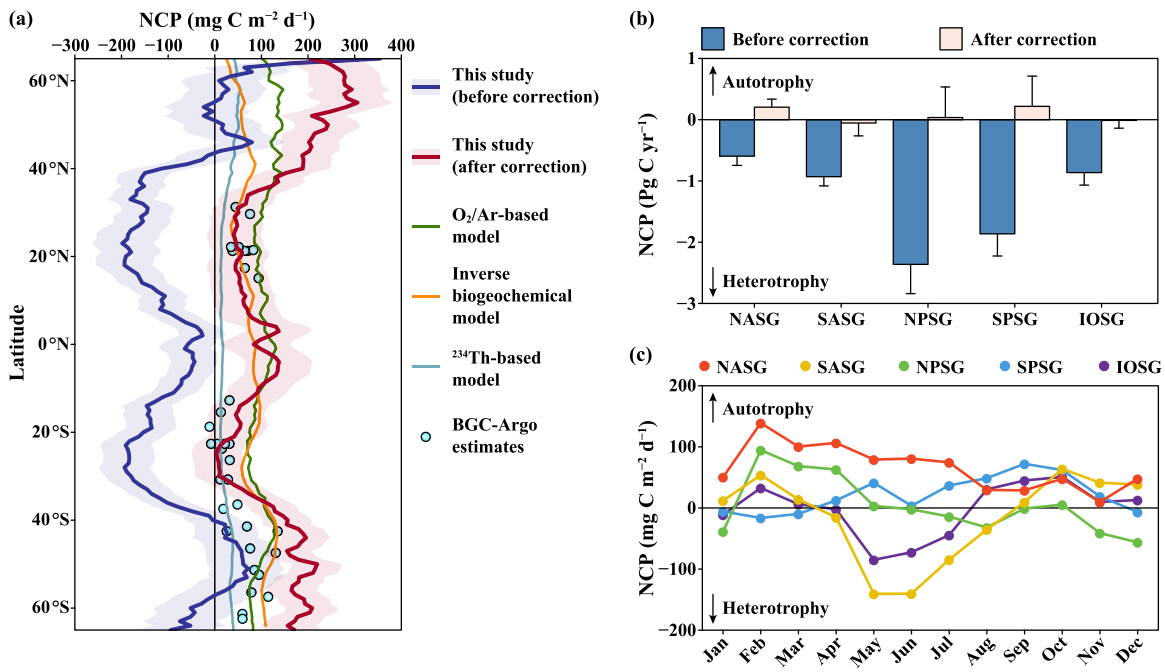

Figure 5. Meridional distribution of net community production (NCP) and spatiotemporal patterns within subtropical oligotrophic gyres. (a) Meridional distribution of annually averaged NCP or carbon export compared with independent model projections and Biogeochemical-Argo field observations. (b) Annual, area-integrated NCP for the five subtropical oligotrophic gyres, shown before (uncorrected) and after the incubation-bias correction. (c) Seasonal evolution of corrected NCP (monthly means) for each gyre. Shading in (a) and error bars in (c) indicate propagated uncertainties in NCP estimates. Gyre acronyms: NASG, North Atlantic Subtropical Gyre; SASG, South Atlantic Subtropical Gyre; NPSG, North Pacific Subtropical Gyre; SPSG, South Pacific Subtropical Gyre; IOSG, Indian Ocean Subtropical Gyre.

Table 1
Comparison of Global Net Community Production (NCP) or Carbon Export Estimates With Prior Studies

Value (Pg C yr^{-1})	Data set	Upscaling	Depth	Reference
-9 ± 2.4	Light-dark bottle incubation	Machine learning	Euphotic zone	This study
12 ± 3.5	Light-dark bottle incubation (corrected for bias)			
−9[a]	Light-dark bottle incubation	PvR linear relationship	Euphotic zone	Westberry et al. (2012)
9[b]	Light-dark bottle incubation (excluding subtropical ocean)			
10	O_2/Ar observations	Machine learning	Mixed layer	Li and Cassar (2016)
15 ± 1.1	Hydrographic data set	Inverse model	73.4 m	Wang et al. (2023)
6	Remote sensing data	Food-web model	Euphotic zone	Siegel et al. (2014)
5	^{234}Th-derived carbon export	Linear relationship	100 m	Henson et al. (2011)

[a]This value was obtained from a reanalysis of the global bottle incubation data set, based on the mean parameters of two production-versus-respiration (PvR) relationships (Duarte & Agustí, 1998; Robinson & Williams, 2005), resulting in an estimated NCP deficit of −782 Tmol C yr^{-1}, equivalent to −9 Pg C yr^{-1}. [b]The refined PvR relationship, derived from global bottle incubation by excluding the data collected in the 10°–40° latitudinal band, estimated an NCP of 781 Tmol C yr^{-1}, equivalent to 9 Pg C yr^{-1}.

tropical and subtropical areas transitioning to net autotrophy (Figures 4 and 5). The metabolic imbalance in oligotrophic oceans is also significantly reduced, with the average euphotic-zone-integrated NCP increasing from -201 ± 95 mg C m^{-2} d^{-1} (uncorrected) to $+12 \pm 74$ mg C m^{-2} d^{-1} (corrected). Globally, correcting for BR bias shifted NCP estimates from an organic carbon deficit of -9 ± 2.4 Pg C yr^{-1} (uncorrected) to a surplus of $+12 \pm 3.5$ Pg C yr^{-1} (65°S–65°N; Table 1).

Under a steady-state assumption, NCP approximates carbon export. After applying the bottle-bias correction, the meridional structure of our revised NCP follows canonical export controls—enhanced at high latitudes and reduced in subtropical gyres—and agrees with independent constraints from an inverse biogeochemical model (Wang et al., 2023), O_2/Ar-based NCP (Li & Cassar, 2016), and profiling-float estimates (Izett et al., 2024) (Figure 5a and Figure S8 in Supporting Information S1). The global area integral likewise falls within the 10–15 Pg C yr^{-1} range indicated using the inverse and O_2/Ar approaches (Table 1). However, our corrected NCP is significantly higher than carbon export estimates derived from ^{234}Th-based method (Henson et al., 2011) or food-web model (Siegel et al., 2014) (5–6 Pg C yr^{-1}; Table 1, Figure 5a and Figure S8 in Supporting Information S1). This discrepancy likely reflects differences in the types of carbon pools accounted for by each method: bottle-based NCP, O_2/Ar ratio, and inverse models account for both dissolved and particulate organic carbon export, while ^{234}Th and food-web models primarily focus on large particulate fluxes, omitting smaller particles and DOC export driven by physical processes such as mixing and eddies (Siegel et al., 2023). Interestingly, our corrected result is also comparable to prior NCP estimates obtained using a refined production-to-respiration (PvR) relationship, which simply excluded data from 10° to 40° latitude (primarily oligotrophic gyres) in the global light-dark bottle data set (Westberry et al., 2012) (9 Pg C yr^{-1}; Table 1). This further supports the conclusion that incubation bias in low-productivity regions is likely primarily due to respiration overestimation driven by enhanced bacterial activity under bottle confinement.

3.4. Emerging Dynamics of Metabolic Balance

Beyond reversing the heterotrophic bias and restoring the expected autotrophic metabolic balance, our correction also enables the detection of more nuanced dynamics in ocean metabolic states that maybe less accessible to traditional tracer budget approaches. NCP derived from tracer budgets typically reflects time-averaged (weeks to months) and area-averaged (hundreds to thousands of kilometers) signals, depending on tracer residence times and the rate of change relative to upper-layer inventory. For example, Yang et al. (2019) demonstrated that NCP inferred from oxygen mass balance integrates signal over ∼100 km on monthly scales, whereas δ^{13}C-DIC mass balance provides an average NCP signal spanning ∼5,000 km over five years. Additionally, chemical tracer mass budgets face challenges in accurately capturing seasonal variations in NCP due to uncertainties in physical mixing parameterization, especially during autumn and winter. Recent comparative studies suggest that NCP meridional gradients inferred from tracer budgets appear less pronounced than those predicted by satellite-based or Earth system model approaches (Emerson, 2014; Quay et al., 2020). While this discrepancy may partially reflect

limitations in empirical algorithms (e.g., inadequate training data sets) or simplifications in process-based models, it also implies potential biases or smoothing effects inherent in tracer-based NCP estimates. In contrast, bottle incubation methods, which directly measure biologically mediated oxygen changes in sealed bottles over a 24-hr period, may more effectively capture the fine-scale variability of metabolic balance in both time and space. These incubations reflect real-time local conditions such as nutrient availability and biological community composition, providing a more detailed and dynamic view of metabolic processes in ocean systems.

Our revised metabolic balance analysis reveals that while area-cumulative corrected NCP values in most gyres approach net autotrophy or metabolic equilibrium (except for the South Atlantic Gyre; Figure 5b and Table S2 in Supporting Information S1), subtropical gyre centers remain slightly net heterotrophic (Figures 4b and 4c). This suggests that organic matter inputs from adjacent regions help balance heterotrophy within gyre centers, making oligotrophic systems largely self-sustaining on a broad scale. Seasonal analyses further highlight shifts between net autotrophy and heterotrophy (Figure 5c), demonstrating the dynamic nature of oligotrophic gyres and the ability of bottle-based methods to capture localized heterotrophic processes. In Northern Hemisphere regions, NCP exhibits a spring maximum followed by a decline in summer. In contrast, in the Southern Hemisphere, different subtropical gyres show distinct behaviors. For example, the South Atlantic Subtropical Gyre exhibits a winter minimum followed by an increase toward austral spring, whereas the South Pacific Subtropical Gyre shows much weaker seasonal variability, consistent with its highly oligotrophic and relatively stable environmental conditions (Emerson & Yang, 2022). While similar seasonal transitions have been observed at a limited number of Biogeochemical-Argo float sites (Yang et al., 2017), our study provides basin-scale confirmation of these patterns. A recent study suggests that heterotrophy in the upper layer does not necessarily preclude particulate organic carbon export, as it may reflect situations where DOC consumption exceeds particulate organic carbon production (Huang, Fassbender, et al., 2022). Notably, certain regions, such as the Mediterranean and South Atlantic gyres, remain predominantly net heterotrophic even after correction (Figures 4b and 4c), likely due to significant terrestrial or riverine organic matter inputs fueling microbial respiration (Duarte et al., 2013; Medeiros et al., 2015). Similarly, enhanced net heterotrophy along the western Pacific gyres may be associated with atmospheric organic carbon deposition from East Asian dust (Duan et al., 2021; Wu et al., 2020), where external inputs stimulate microbial respiration, leading to localized carbon consumption exceeding autotrophic production.

Our study could also help explain another long-standing paradox regarding the imbalance between carbon export and mesopelagic carbon demand. We compared our revised NCP estimates with in situ data from three well-established time-series stations—ALOHA, K2, and PAP—where sinking particulate organic carbon fluxes are reported to be insufficient to sustain mesopelagic CR (Giering et al., 2014; Steinberg et al., 2008). As discussed earlier, our bottle-incubation estimates include both upper layer export potential attributed to dissolved and particulate phases. Correcting for BR bias revealed that surplus organic carbon from the upper ocean can balance mesopelagic CR and support carbon sequestration (Table S3 in Supporting Information S1). In contrast, uncorrected NCP balanced mesopelagic CR only at K2, likely due to its location outside oligotrophic gyres and lower susceptibility to bottle effects, while at ALOHA and PAP, it was insufficient to meet even euphotic carbon demand (Table S3 in Supporting Information S1). This underscores the importance of refining metabolic balance assessments for accurate oceanic carbon budget estimates.

3.5. Limitations and Caveats of the Correction Framework

While the proposed framework provides a first-order correction for incubation-induced bias in respiration estimates, several limitations should be acknowledged. These can be broadly grouped into (a) simplifying assumptions in the correction framework, and (b) other sources contributing to the corrected NCP estimates.

3.5.1. Assumptions in the Correction Framework

The correction framework relies on several simplifying assumptions, yet these are expected to exert only a limited first-order impact. First, the correction framework assumes an exponential bacterial growth model, using BP measurements at the beginning and end of the incubation to estimate time-integrated activity over 24 hr. The validity of this assumption is supported by high-frequency observations at selected stations (Figure S2 in Supporting Information S1), which are consistent with well-established exponential growth behavior in marine bacteria (Guo et al., 2022; Pomeroy et al., 1994). Additional uncertainty arises from conversion factors used in

leucine-based BP estimates. In this study, we applied conversion factors that were accurately determined in previous studies conducted in the same region (Huang et al., 2019; Wang et al., 2014). Importantly, theoretical derivations (Text S3 in Supporting Information S1) demonstrate that the conversion factor cancels out in the calculation of respiration overestimation. Therefore, the final correction is independent of the specific choice of conversion factor.

Second, the framework links incubation-enhanced BP to excess respiration using a first-order approximation constrained by BGE. Site-specific BGE was obtained using size-fractionated filtration (<0.8 μm) to isolate bacterial communities for independent BP and BR measurements, combined with an exponential growth model to reconstruct time-integrated BP and correct for incubation-induced enhancement of bacterial activity (Text S1 in Supporting Information S1). Compared with traditional approaches or literature-based empirical estimates, this improved method ensures temporal consistency between BP and BR and better captures local carbon allocation regimes. It is worth noting that this framework assumes constant BGE during incubation, an assumption also adopted in previous incubation-based correction studies (Guo et al., 2022). To evaluate the validity of this assumption, we conducted additional incubation experiments at selected stations and applied an independent approach to quantify BR during the initial phase of incubation (Text S2 in Supporting Information S1). We found that the measured initial BR activity was in good agreement with respiration rates theoretically inferred under the assumption of constant BGE (Figure S10 in Supporting Information S1). This consistency provides empirical support for the assumption that BGE remains relatively stable during the incubation period.

Finally, due to prefiltration (<0.8 μm), our BGE measurements primarily represent free-living heterotrophic bacteria and exclude most particle-associated bacterial activity. In the upper ocean, particle-attached bacteria typically account for a relatively small fraction of total bacterial biomass, generally <15% in coastal systems and lower offshore (Del Giorgio et al., 2011; Guo et al., 2022). Although these bacteria may exhibit higher cell-specific metabolic rates, their exclusion is expected to have a limited impact on respiration estimates of the overall bacterial community, particularly in the open ocean, which comprises most of the global ocean.

3.5.2. Second-Order Sources of Uncertainty

Additional sources of uncertainty include those associated with extrapolation, contributions from other respiratory components, and reliance on empirical relationships in the absence of fully resolved mechanisms. Together, these factors introduce second-order uncertainties in the correction of global respiration and, consequently, the derived metabolic balance.

To begin with, extrapolation of empirically derived relationships introduces uncertainties. The correction framework was parameterized using a limited number of incubation experiments (Figure 1) and applied across diverse environmental and vertical domains. Although our measurements span a broad range of conditions, certain regimes—particularly high-latitudes and strongly seasonal environments—remain underrepresented. Meanwhile, the relationships were derived primarily from surface observations and applied uniformly throughout the water column, implicitly assuming vertical invariance. The global light-dark bottle data set used for large-scale NCP extrapolation is also unevenly distributed in space and time (Figure 1c), introducing additional uncertainty in under sampled regions and seasons. Nevertheless, the corrected global NCP patterns are broadly consistent with independent constraints, including remote sensing algorithms and biogeochemical models (Table 1 and Figure 5a), suggesting that the framework likely captures a systematic bias rather than site-specific variability (see Text S4 in Supporting Information S1 for details).

In addition, the framework is empirical and does not explicitly resolve the mechanisms underlying incubation-induced changes in bacterial activity. Such changes likely emerge from multiple interacting processes that are difficult to constrain explicitly, particularly in small-volume bottle incubations. These processes may include variations in DOC availability and quality, omission of respiration attributed by particle-associated bacteria, shifts in phytoplankton physiology (e.g., suppression of light-dependent processes and the absence of photorespiration under dark conditions), changes in microbial community structure, and trophic interactions (Baltar et al., 2012; Bender et al., 1987; Calvo-Diaz et al., 2011; Guo et al., 2022; Westberry et al., 2012). While these processes may modulate the magnitude of the bias across ecosystems—and in some cases partially offset the overestimation of BR—they remain insufficiently constrained. Accordingly, they are treated as second-order sources of uncertainty that affect the magnitude, but not the dominant first-order pattern, of the corrected estimates (see Text S5 in Supporting Information S1 for further discussion).

Future work integrating observations of DOC composition, microbial community structure, phytoplankton physiology, particle-associated bacteria, and trophic interactions, together with time-resolved measurements of metabolic processes, will be essential for developing more mechanistic and regionally resolved correction frameworks. In this context, the present study establishes a first-order correction framework while highlighting pathways for further refinement.

4. Conclusion

This study provides a new explanation for the long-standing discrepancy between bottle incubation-based and incubation-free estimates of ocean metabolic balance. By quantifying the enhancement of bacterial activity during incubation and applying a correction framework, we show that oligotrophic regions are more likely to be net autotrophic than previously inferred from uncorrected bottle measurements. The corrected estimates lead to a more internally consistent view of the ocean carbon cycle, reducing the apparent imbalance between upper-ocean organic carbon production and mesopelagic carbon demand. By retaining the high spatial and temporal resolution of bottle incubations while accounting for systematic biases, this framework provides an improved observational constraint on metabolic balance and offers a pathway for integrating incubation-based measurements into large-scale assessments of ocean carbon cycling.

Conflict of Interest

The authors declare no conflicts of interest relevant to this study.

Availability Statement

Field experiment data and the compiled global light-dark bottle data set are provided by Liu et al. (2025). Bacterial abundance data used for respiration correction can be accessed from Buitenhuis et al. (2012). Environmental predictors used in the machine-learning framework for global net community production estimation, including temperature, salinity, DO, nutrients, mixed-layer depth, sea-surface chlorophyll, and primary production data, can be accessed from Liu (2026). Net community production based on Biogeochemical-Argo observations is extracted from published figures in Izett et al. (2024). Mesopelagic CR at three typical time-series stations was obtained from Giering et al. (2014) and Steinberg et al. (2008). All analysis scripts are openly available in the GitHub repository: https://github.com/LiuXYh/BR_NCP.

Acknowledgments

This work was supported by the National Natural Science Foundation of China (Grant 42130401, 42406099), Natural Science Foundation of Xiamen, China (Grant 3502Z202472006), Natural Science Foundation of Fujian Province, China (No. 2025J09005), and Fundamental Research Funds for the Central Universities (Grant 20720240105 and 20720240053). We thank the Ocean Carbon Group in the State Key Laboratory of Marine Environmental Science at Xiamen University and the Fujian Institute of Oceanography for providing environmental factor data from the field experiments. We also extend our gratitude to the captain and crew of the R/V *Yanping II* and *Tan Kah Kee* for their cooperation during the field cruises.

References

Alotaibi, G. F. (2021). Factors influencing bacterial biofilm formation and development. *American Journal of Biomedical Science & Research*, *12*(6), 617–626. https://doi.org/10.34297/ajbsr.2021.12.001820

Azam, F. (1998). Microbial control of Oceanic carbon flux: The plot thickens. *Science*, *280*(5364), 694–696. https://doi.org/10.1126/science.280.5364.694

Baltar, F., Lindh, M. V., Parparov, A., Berman, T., & Pinhassi, J. (2012). Prokaryotic community structure and respiration during long-term incubations. *MicrobiologyOpen*, *1*(2), 214–224. https://doi.org/10.1002/mbo3.25

Baumas, C. M. J., Le Moigne, F. A. C., Garel, M., Bhairy, N., Guasco, S., Riou, V., et al. (2021). Mesopelagic microbial carbon production correlates with diversity across different marine particle fractions. *ISME Journal*, *15*(6), 1695–1708. https://doi.org/10.1038/s41396-020-00880-z

Bender, M., Grande, K., Johnson, K., Marra, J., Williams, P. J. L., Sieburth, J., et al. (1987). A comparison of four methods for determining planktonic community production. *Limnology and Oceanography*, *32*(5), 1085–1098. https://doi.org/10.4319/lo.1987.32.5.1085

Buitenhuis, E., Li, W., Lomas, M., Karl, D., Landry, M., & Jacquet, S. (2012). Picoheterotroph (bacteria and archaea) biomass distribution in the global ocean. *Earth System Science Data*, *4*(1), 101–106. https://doi.org/10.5194/essd-4-101-2012

Burd, A. B., Hansell, D. A., Steinberg, D. K., Anderson, T. R., Arístegui, J., Baltar, F., et al. (2010). Assessing the apparent imbalance between geochemical and biochemical indicators of meso- and bathypelagic biological activity: What the @$♯! is wrong with present calculations of carbon budgets? *Deep Sea Research Part II: Topical Studies in Oceanography*, *57*(16), 1557–1571. https://doi.org/10.1016/j.dsr2.2010.02.022

Calvo-Diaz, A., Diaz-Perez, L., Suarez, L. A., Moran, X. A., Teira, E., & Maranon, E. (2011). Decrease in the autotrophic-to-heterotrophic biomass ratio of picoplankton in oligotrophic marine waters due to bottle enclosure. *Applied and Environmental Microbiology*, *77*(16), 5739–5746. https://doi.org/10.1128/AEM.00066-11

Dai, M., Luo, Y. W., Achterberg, E. P., Browning, T. J., Cai, Y., Cao, Z., et al. (2023). Upper ocean biogeochemistry of the oligotrophic north Pacific subtropical gyre: From nutrient sources to carbon export. *Reviews of Geophysics*, *61*(3), e2022RG000800. https://doi.org/10.1029/2022RG000800

Del Giorgio, P. A., Condon, R., Bouvier, T., Longnecker, K., Bouvier, C., Sherr, E., & Gasol, J. M. (2011). Coherent patterns in bacterial growth, growth efficiency, and leucine metabolism along a northeastern Pacific inshore-offshore transect. *Limnology and Oceanography*, *56*(1), 1–16. https://doi.org/10.4319/lo.2011.56.1.0001

DeVries, T. (2022). The ocean carbon cycle. *Annual Review of Environment and Resources*, *47*(1), 317–341. https://doi.org/10.1146/annurev-environ-120920-111307

Duan, X., Guo, C., Zhang, C., Li, H., Zhou, Y., Gao, H., et al. (2021). Effect of East Asian atmospheric particulate matter deposition on bacterial activity and community structure in the oligotrophic northwest Pacific. *Environmental Pollution*, *283*, 117088. https://doi.org/10.1016/j.envpol.2021.117088

Duarte, C. M., & Agustí, S. (1998). The CO_2 balance of unproductive aquatic ecosystems. *Science*, *281*(5374), 234–236. https://doi.org/10.1126/science.281.5374.234

Duarte, C. M., Regaudie-de-Gioux, A., Arrieta, J. M., Delgado-Huertas, A., & Agusti, S. (2013). The oligotrophic ocean is heterotrophic. *Annual Review of Marine Science*, *5*(1), 551–569. https://doi.org/10.1146/annurev-marine-121211-172337

Ducklow, H. W., & Doney, S. C. (2013). What is the metabolic state of the oligotrophic ocean? A debate. *Annual Review of Marine Science*, *5*(1), 525–533. https://doi.org/10.1146/annurev-marine-121211-172331

Emerson, S. (2014). Annual net community production and the biological carbon flux in the ocean. *Global Biogeochemical Cycles*, *28*(1), 14–28. https://doi.org/10.1002/2013gb004680

Emerson, S., & Yang, B. (2022). The ocean's biological pump: In situ oxygen measurements in the subtropical oceans. *Geophysical Research Letters*, *49*(21), e2022GL099834. https://doi.org/10.1029/2022GL099834

Falkowski, P., Scholes, R. J., Boyle, E., Canadell, J., Canfield, D., Elser, J., et al. (2000). The global carbon cycle: A test of our knowledge of Earth as a system. *Science*, *290*(5490), 291–296. https://doi.org/10.1126/science.290.5490.291

García-Martín, E. E., Aranguren-Gassis, M., Hartmann, M., Zubkov, M. V., & Serret, P. (2017). Contribution of bacterial respiration to plankton respiration from 50°N to 44°S in the Atlantic Ocean. *Progress in Oceanography*, *158*, 99–108. https://doi.org/10.1016/j.pocean.2016.11.006

Giering, S. L., Sanders, R., Lampitt, R. S., Anderson, T. R., Tamburini, C., Boutrif, M., et al. (2014). Reconciliation of the carbon budget in the ocean's twilight zone. *Nature*, *507*(7493), 480–483. https://doi.org/10.1038/nature13123

Gómez-Consarnau, L., Raven, J. A., Levine, N. M., Cutter, L. S., Wang, D., Seegers, B., et al. (2019). Microbial rhodopsins are major contributors to the solar energy captured in the sea. *Science Advances*, *5*(8), eaaw8855. https://doi.org/10.1126/sciadv.aaw8855

Guo, C., Ke, Y., Chen, B., Zhang, S., & Liu, H. (2022). Making comparable measurements of bacterial respiration and production in the subtropical coastal waters. *Marine Life Science and Technology*, *4*(3), 414–427. https://doi.org/10.1007/s42995-022-00133-2

Heneghan, R. F., Holloway-Brown, J., Gasol, J. M., Herndl, G. J., Moran, X. A. G., & Galbraith, E. D. (2024). The global distribution and climate resilience of marine heterotrophic prokaryotes. *Nature Communications*, *15*(1), 6943. https://doi.org/10.1038/s41467-024-50635-z

Henson, S. A., Sanders, R., Madsen, E., Morris, P. J., Le Moigne, F., & Quartly, G. D. (2011). A reduced estimate of the strength of the ocean's biological carbon pump. *Geophysical Research Letters*, *38*(4), L04606. https://doi.org/10.1029/2011gl046735

Huang, Y., Chen, B., Huang, B., Zhou, H., & Yuan, Y. (2019). Potential overestimation of community respiration in the western Pacific boundary ocean: What causes the putative net heterotrophy in oligotrophic systems? *Limnology and Oceanography*, *64*(5), 2202–2219. https://doi.org/10.1002/lno.11179

Huang, Y., Eveleth, R., Nicholson, D., & Cassar, N. (2022). Can we estimate air-sea flux of biological O_2 from total dissolved oxygen? *Global Biogeochemical Cycles*, *36*(9), e2021GB007145. https://doi.org/10.1029/2021GB007145

Huang, Y., Fassbender, A. J., & Bushinsky, S. M. (2023). Biogenic carbon pool production maintains the Southern Ocean carbon sink. *Proceedings of the National Academy of Sciences*, *120*(18), e2217909120. https://doi.org/10.1073/pnas.2217909120

Huang, Y., Fassbender, A. J., Long, J. S., Johannessen, S., & Bernardi Bif, M. (2022). Partitioning the export of distinct biogenic carbon pools in the northeast Pacific Ocean using a biogeochemical profiling float. *Global Biogeochemical Cycles*, *36*(2), e2021GB007178. https://doi.org/10.1029/2021gb007178

Huang, Y., Nicholson, D., Huang, B., & Cassar, N. (2021). Global estimates of marine gross primary production based on machine learning opscaling of field observations. *Global Biogeochemical Cycles*, *35*(3), e2020GB006718. https://doi.org/10.1029/2020gb006718

Izett, R. W., Fennel, K., Stoer, A. C., & Nicholson, D. P. (2024). Reviews and syntheses: Expanding the global coverage of gross primary production and net community production measurements using Biogeochemical-argo floats. *Biogeosciences*, *21*(1), 13–47. https://doi.org/10.5194/bg-21-13-2024

Kirchman, D. (2001). Measuring bacterial biomass production and growth rates from leucine incorporation in natural aquatic environments. *Methods in Microbiology*, *30*, 227–237. https://doi.org/10.1016/S0580-9517(01)30047-8

Laws, E. A. (1991). Photosynthetic quotients, new production and net community production in the open ocean. *Deep Sea Research Part I: Oceanographic Research Papers*, *38*(1), 143–167. https://doi.org/10.1016/0198-0149(91)90059-O

Li, Z., & Cassar, N. (2016). Satellite estimates of net community production based on O_2/Ar observations and comparison to other estimates. *Global Biogeochemical Cycles*, *30*(5), 735–752. https://doi.org/10.1002/2015gb005314

Liu, Y. (2026). Climatological surface environmental parameters and primary production for the 1° global ocean grid [Dataset]. *Zenodo*. https://doi.org/10.5281/zenodo.19694236

Liu, Y., Huang, Y., & Huang, B. (2025). Global net community production dataset from light-dark bottle incubations [Dataset]. *Zenodo*. https://doi.org/10.5281/zenodo.15186268

Marie, D., Simon, N., & Vaulot, D. (2005). Phytoplankton cell counting by flow cytometry. *Algal Culturing Techniques*, *1*, 253–267. https://doi.org/10.1016/B978-012088426-1/50018-4

Massana, R., Pedrós-Alió, C., Casamayor, E. O., & Gasol, J. M. (2001). Changes in marine bacterioplankton phylogenetic composition during incubations designed to measure biogeochemically significant parameters. *Limnology and Oceanography*, *46*(5), 1181–1188. https://doi.org/10.4319/lo.2001.46.5.1181

Medeiros, P. M., Seidel, M., Ward, N. D., Carpenter, E. J., Gomes, H. R., Niggemann, J., et al. (2015). Fate of the amazon river dissolved organic matter in the tropical Atlantic Ocean. *Global Biogeochemical Cycles*, *29*(5), 677–690. https://doi.org/10.1002/2015gb005115

Mojica, K. D., Huisman, J., Wilhelm, S. W., & Brussaard, C. P. (2016). Latitudinal variation in virus-induced mortality of phytoplankton across the north Atlantic Ocean. *ISME Journal*, *10*(2), 500–513. https://doi.org/10.1038/ismej.2015.130

Moran, M. A., Ferrer-González, F. X., Fu, H., Nowinski, B., Olofsson, M., Powers, M. A., et al. (2022). The ocean's labile DOC supply chain. *Limnology and Oceanography*, *67*(5), 1007–1021. https://doi.org/10.1002/lno.12053

Morán, X. A. G., Pérez, V., & Fernández, E. (2007). Mismatch between community respiration and the contribution of heterotrophic bacteria in the NE Atlantic open ocean: What causes high respiration in oligotrophic waters? *Journal of Marine Research*, *65*(4), 545–560. https://doi.org/10.1357/002224007782689102

Munson-McGee, J. H., Lindsay, M. R., Sintes, E., Brown, J. M., D'Angelo, T., Brown, J., et al. (2022). Decoupling of respiration rates and abundance in marine prokaryoplankton. *Nature*, *612*(7941), 764–770. https://doi.org/10.1038/s41586-022-05505-3

Pierella Karlusich, J. J., Ibarbalz, F. M., & Bowler, C. (2020). Phytoplankton in the tara ocean. *Annual Review of Marine Science*, *12*(1), 233–265. https://doi.org/10.1146/annurev-marine-010419-010706

Pomeroy, L. R., Sheldon, J. E., & Sheldon, W. M.Jr. (1994). Changes in bacterial numbers and leucine assimilation during estimations of microbial respiratory rates in seawater by the precision winkler method. *Applied and Environmental Microbiology*, *60*(1), 328–332. https://doi.org/10.1128/aem.60.1.328-332.1994

Qian, P. Y., Cheng, A., Wang, R., & Zhang, R. (2022). Marine biofilms: Diversity, interactions and biofouling. *Nature Reviews Microbiology*, *20*(11), 671–684. https://doi.org/10.1038/s41579-022-00744-7

Quay, P., Emerson, S., & Palevsky, H. (2020). Regional pattern of the ocean's biological pump based on geochemical observations. *Geophysical Research Letters*, *47*(14), e2020GL088098. https://doi.org/10.1029/2020gl088098

Robinson, C., & Williams, P. l. B. (2005). Respiration and its measurement in surface marine waters. In *Respiration in aquatic ecosystems* (pp. 147–180). Oxford University Press.

Serret, P., Fernández, E., & Robinson, C. (2002). Biogeographic differences in the net ecosystem metabolism of the open ocean. *Ecology*, *83*(11), 3225–3234. https://doi.org/10.1890/0012-9658(2002)083[3225:BDITNE]2.0.CO;2

Serret, P., Robinson, C., Fernández, E., Teira, E., & Tilstone, G. (2001). Latitudinal variation of the balance between plankton photosynthesis and respiration in the eastern Atlantic Ocean. *Limnology and Oceanography*, *46*(7), 1642–1652. https://doi.org/10.4319/lo.2001.46.7.1642

Siegel, D. A., Buesseler, K. O., Doney, S. C., Sailley, S. F., Behrenfeld, M. J., & Boyd, P. W. (2014). Global assessment of ocean carbon export by combining satellite observations and food-web models. *Global Biogeochemical Cycles*, *28*(3), 181–196. https://doi.org/10.1002/2013gb004743

Siegel, D. A., DeVries, T., Cetinic, I., & Bisson, K. M. (2023). Quantifying the ocean's biological pump and its carbon cycle impacts on global scales. *Annual Review of Marine Science*, *15*(1), 329–356. https://doi.org/10.1146/annurev-marine-040722-115226

Steinberg, D. K., Van Mooy, B. A. S., Buesseler, K. O., Boyd, P. W., Kobari, T., & Karl, D. M. (2008). Bacterial vs. zooplankton control of sinking particle flux in the ocean's twilight zone. *Limnology and Oceanography*, *53*(4), 1327–1338. https://doi.org/10.4319/lo.2008.53.4.1327

Wang, N., Lin, W., Chen, B., & Huang, B. (2014). Metabolic states of the Taiwan strait and the northern South China Sea in summer 2012. *Journal of Tropical Oceanography*, *33*(4), 61–68. https://doi.org/10.3969/j.issn.1009-5470.2014.04.008

Wang, W. L., Fu, W., Le Moigne, F. A. C., Letscher, R. T., Liu, Y., Tang, J. M., & Primeau, F. W. (2023). Biological carbon pump estimate based on multidecadal hydrographic data. *Nature*, *624*(7992), 579–585. https://doi.org/10.1038/s41586-023-06772-4

Westberry, T. K., Williams, P. J. l. B., & Behrenfeld, M. J. (2012). Global net community production and the putative net heterotrophy of the oligotrophic oceans. *Global Biogeochemical Cycles*, *26*(4), GB4019. https://doi.org/10.1029/2011gb004094

Williams, P. J. l. B., Morris, P. J., & Karl, D. M. (2004). Net community production and metabolic balance at the oligotrophic ocean site, station ALOHA. *Deep Sea Research Part I: Oceanographic Research Papers*, *51*(11), 1563–1578. https://doi.org/10.1016/j.dsr.2004.07.001

Williams, P. J. l. B., Quay, P. D., Westberry, T. K., & Behrenfeld, M. J. (2013). The oligotrophic ocean is autotrophic. *Annual Review of Marine Science*, *5*(1), 535–549. https://doi.org/10.1146/annurev-marine-121211-172335

Wu, Z., Hu, L., Guo, T., Lin, T., & Guo, Z. (2020). Aeolian transport and deposition of carbonaceous aerosols over the northwest Pacific Ocean in spring. *Atmospheric Environment*, *223*, 117209. https://doi.org/10.1016/j.atmosenv.2019.117209

Yang, B., Emerson, S. R., & Bushinsky, S. M. (2017). Annual net community production in the subtropical Pacific Ocean from *In Situ* oxygen measurements on profiling floats. *Global Biogeochemical Cycles*, *31*(4), 728–744. https://doi.org/10.1002/2016gb005545

Yang, B., Emerson, S. R., & Quay, P. D. (2019). The subtropical ocean's biological carbon pump determined from O_2 and DIC/DI^{13}C tracers. *Geophysical Research Letters*, *46*(10), 5361–5368. https://doi.org/10.1029/2018gl081239

Yu, X., Wen, Z., Jiang, R., Yang, J. Y. T., Cao, Z., Hong, H., et al. (2024). Assessing N_2 fixation flux and its controlling factors in the (sub)tropical Western north Pacific through high-resolution observations. *Limnology and Oceanography Letters*, *9*(6), 716–724. https://doi.org/10.1002/lol2.10404